



SIXTH FRAMEWORK PROGRAMME

MESOR

Management and Exploitation of Solar Resource Knowledge

CA - Contract No. 038665

D 1.2.1 & D1.2.2

Description of solar resource products

Summary of benchmarking results

Examples of use

Dominique Dumortier, ENTPE



Date: 30-06-2009

Version History

Version	Date	Authors	Partner	Sent To	Major Changes
1.0	2009-06-30	D. Dumortier	ENTPE	Consortium	Initial version
1.1	2009-08-25	D. Dumortier M. Suri C. Hoyer-Click	ENTPE GeoModel DLR	Consortium	New maps for GHI spatial comparison

Table of Contents

1	Introduction.....	4
2	Description of solar resource products	4
2.1	Provider, input data, area and time period	4
2.2	Spatial and temporal resolutions	4
2.3	Parameters.....	5
2.4	Detailed computation methods	5
3	Main results of MESOR benchmarking.....	7
3.1	Global horizontal irradiance	7
3.2	Direct normal irradiance.....	15
4	References	21
5	Examples of use	23

1 Introduction

This report has three parts. The first one provides a description of the solar radiation resource products covering Europe. The second one presents the results of the benchmarking done within MESOR for some of these products. The third one presents best case studies which show how solar radiation data is being used by practitioners.

2 Description of solar resource products

2.1 *Provider, input data, area and time period*

Product	Provider	Input data	Area	Time period
ENMETSOL	Univ. Oldenburg, Germany	Satellite	Europe, Africa	Since 1995
ESRA	Mines Paris-Tech, France (www.helioclim.net)	Ground	Europe	1981-1990
HELIOCLIM	Mines Paris-Tech, France (www.helioclim.net)	Satellite	Europe, Africa	Since 1985
METEONORM 6	Meteotest, Switzerland (www.meteonorm.com)	Ground + Satellite	World	1981-2000
NASA SSE 6	NASA, USA (eosweb.larc.nasa.gov/sse)	ISCCP	World	1983-2005
PVGIS Europe	JRC, Italy (re.jrc.ec.europa.eu/pvgis)	Ground	Europe	1981-1990
SATEL-LIGHT	ENTPE, France (www.satel-light.com)	Satellite	West and Central Europe	1996-2000
SOLEMI	DLR, Germany (www.solemi.com)	Satellite	Europe, Africa, West Asia	Since 1991

ISCCP stands for International Satellite Cloud Climatology Project.

Table 1: Solar resource products: provider, area and time period coverage.

2.2 *Spatial and temporal resolutions*

Product	Spatial resolution	Temporal resolution
ENMETSOL	3-7 km//1-3 km	15mn/1h
ESRA	10 km	Average daily profile
HELIOCLIM	30 km//3-7 km	15mn/30mn
METEONORM 6	1 km (+90 m disaggregation)	Average daily profile (1mn/1h)
NASA SSE 6	100 km	Average daily profile
PVGIS Europe	1 km (+90 m disaggregation)	Average daily profile
SATEL-LIGHT	5-7 km	30mn
SOLEMI	1 km	1h

The 90 m disaggregation is based on the Shuttle Radar Topography Mission data (SRTM).

Table 2: Solar resource products: spatial and temporal resolutions.

2.3 Parameters

All the products provide irradiance; this is the rate at which radiant energy is incident on a surface, per unit area of the surface. The unit is W/m². GHI is the global horizontal irradiance: the irradiance from the sun and the sky vault on a horizontal surface. DHI is the diffuse horizontal irradiance: the irradiance from the sky vault on a horizontal surface. DNI is the direct normal irradiance: the irradiance from the sun on a surface perpendicular to the sun.

Some products also provide illuminance; it is the same as irradiance except that the radiant energy is evaluated according to its action on the human eye defined by the CIE standard photometric observer. Its unit is lux. Illuminances are used by architects or engineers to make sure that daylight or electric light levels in buildings correspond to the needs of human vision.

Some products provide the spectrum of solar radiation, irradiances and/or illuminances on inclined surfaces and some are able to take into account the effect of high horizon (terrain shadowing).

Product	Parameters
ENMETSOL	GHI, DHI, DNI, Spectrum
ESRA	GHI, DHI, DNI, Inclined surfaces
HELIOCLIM	GHI, DNI
METEONORM 6	GHI, DHI, DNI, Inclined surfaces, Shadowing, Illuminances
NASA SSE 6	GHI, DHI, DNI, Inclined surfaces, Clouds
PVGIS Europe	GHI, DHI, Inclined surfaces, Shadowing
SATEL-LIGHT	GHI, DHI, DNI, Inclined surfaces, Illuminances
SOLEMI	GHI, DNI

Table 3: Solar resource products: parameters available.

2.4 Detailed computation methods

Product	Global horizontal irradiance	Diffuse horizontal irradiance	Diffuse on inclined surface	Simulation of time series
ENMETSOL	Heliosat-3 cloud index model from Hammer (2007). Clear sky model: v1 from Dumortier (1995), v2 : from Müller (2004)]	Diffuse fraction model: v1 from Skartveit (1998), v2 from Kemper (2008).	n/a	Real 60mn or 15mn data.
ESRA	Interpolation of ground data by krigging from Beyer (1997).	63 of 560 measured, the remaining estimated by Czeplak (1996)	Model from Muneer (1990).	Simulation of daily average profile by Collares-Pereira (1979) and Liu (1960).

HELIOCLIM	Heliosat-2 cloud index model from Rigollier (2004).	n/a	n/a	Real 15mn data.
METEONORM 6	Heliosat-1 for satellite data; Ground data interpolation from Zelenka (1992) and Wald (2001).	Diffuse fraction model from Perez (1991).	Model from Perez (1987) with obstruction effect described by Remund (1998).	Simulation of daily, hourly and minute values from monthly averages by Aguiar (1988) and Collares-Pereira (1992)
NASA SSE 6	Satellite model by Pinker (1992). NASA ISCCP & CERES MODIS irradiance, clouds and surface parameters; NCAR MATCH aerosols; TOMS/TOVS ozone; NASA/GMAO GEOS-4 surface parameters	Diffuse fraction model from Erbs (1982).	Retscreen method based on Duffie & Beckman (1991).	Simulation of daily average profile by Collares-Pereira (1979) and Liu (1960)
PVGIS Europe	3D spline interpolation of ground data + model <i>r. sun</i> from Suri (2004).	63 of 560 measured, the remaining estimated by Czeplak (1996).	Model from Muneer (1990).	Simulation of daily average profile from monthly averages using diffuse and beam clear-sky coefficients by Suri (2004).
SATEL-LIGHT	Heliosat-2 cloud index model from Hammer (2003). Clear sky model: from Dumortier (1995) with Linke turbidity from Remund (2003).	Diffuse fraction model from Skartveit (1998)	Model from Skartveit (1986)	Real 30mn data
SOLEMI	Bird clear sky model. Heliosat2 cloud index with new cloud transmission functions. NASA GISS aerosols, NCAR/NCEP water vapour, TOMS ozone	n/a	n/a	Real 60mn data

Complete references for the models used in the products are in the references section.

Table 4: Solar resource products: computation methods.

3 Main results of MESOR benchmarking

Benchmarking solar radiation products was an important task of the MESOR project. Our approach was twofold: first a site comparison using ground measurements, second a large scale comparison between products over Europe. The main results are presented below. They are fully described in deliverable D1.1.3. Because high quality hourly measurements of solar radiation from the ground are rather scarce, we have only been able to gather measurements from 10 sites in Europe. Figure 1 shows the location of each site as well as the period of time used for the benchmarking. The measurements have gone through the MESOR quality control procedure which is fully described in deliverable D.1.1.2.

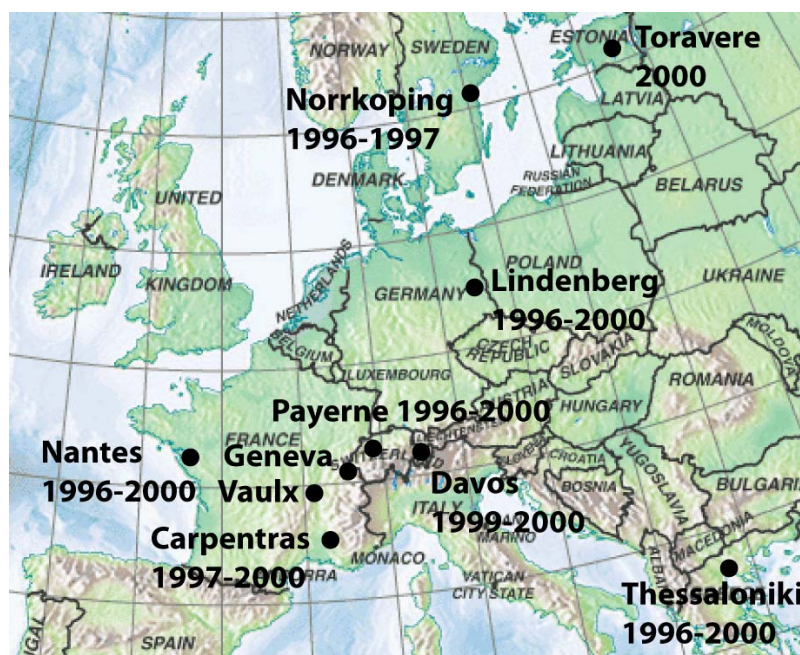


Figure 1: Ground measurement sites used for the benchmarking.

The MESOR benchmarking was done not only for the global horizontal irradiance (GHI) but also for the direct normal irradiance (DNI) which is important for solar concentrating systems. The comparison to ground measurements looked at the match between hourly time series while the large scale comparison over Europe looked at yearly sums of the irradiation.

We used well know statistic measures such as the bias and the root mean square deviation (RMSD). They show how well data pairs at the same point of time compare with each other. They are important if one needs an exact representation of real data, e.g. for evaluations of real operating systems or forecasts of solar radiation parameters. However, for system design, the similarity of frequency distributions is more important. Therefore, we added another statistic called the Kolmogorov-Smirnov Integral (KSI) [Polo, 2009] which is used to measure the difference between frequency distributions. KSI is below 100% when frequency distributions are close to each other.

3.1 Global horizontal irradiance

Figure 2 gives the average hourly global horizontal irradiance (GHI) obtained from the ground measurements. Payerne is the site where the average GHI is the highest followed by Carpentras and Thessaloniki. Toravere and Norrköping with high latitudes have the lowest average GHI.

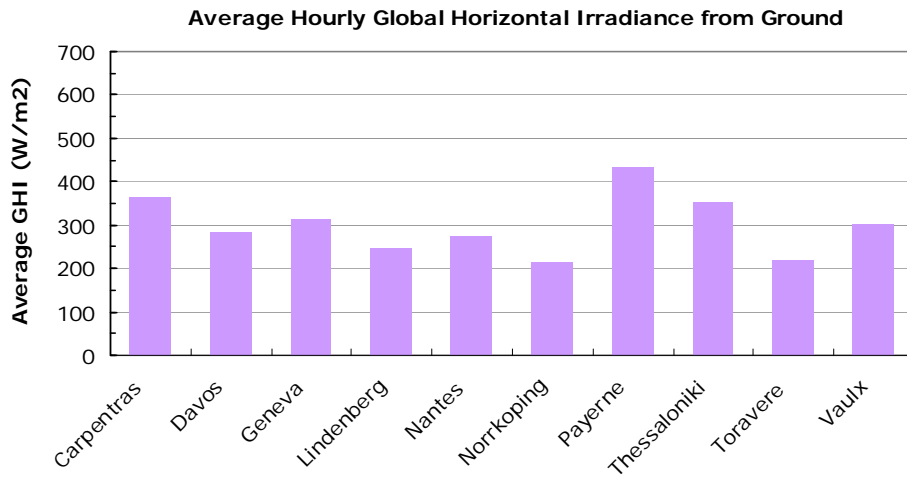


Figure 2: Average GHI for the benchmarking period (ground measurements).

The next 3 figures present the bias, the RMSD and the KSI obtained from the comparison between 3 solar resource products (ENMETSOL, SATEL-LIGHT, SOLEMI) and the ground measurements.

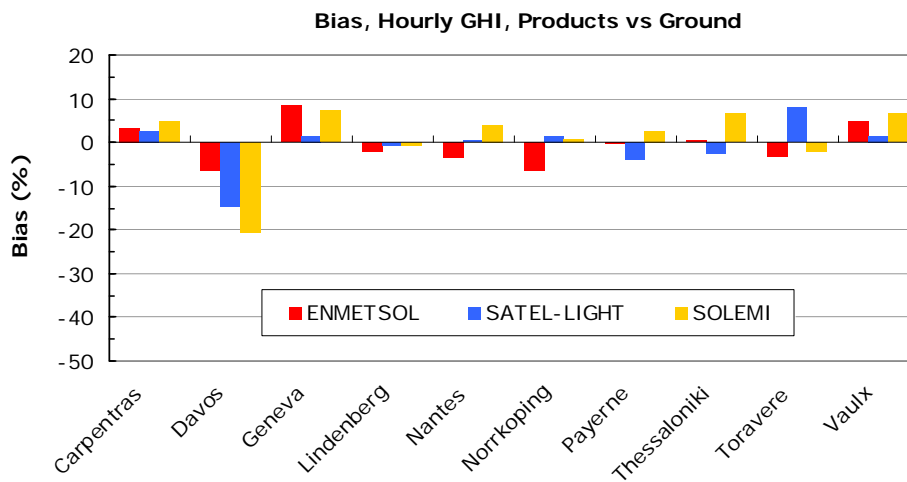


Figure 3: Bias between ground measurements and 3 products.

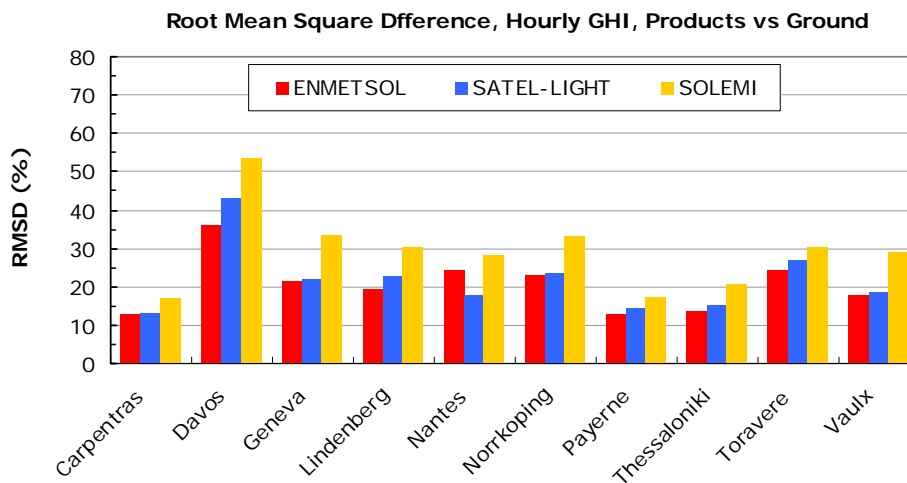


Figure 4: RMSD between ground measurements and 3 products.

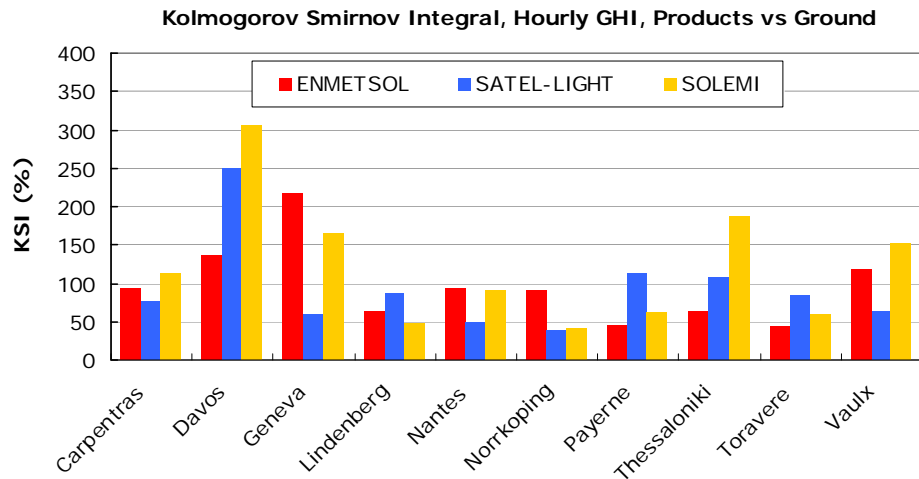


Figure 5: KSI between ground measurements and 3 products.

The overall bias is low for all data bases, 3% for SOLEMI, -1% for SATEL-LIGHT and 1% for ENMETSOL. For each product, there is no general trend from one site to another, one product may either under-estimate or over-estimate GHI. The only exception is Davos where all products under-estimate the global irradiance. This is due to snow coverage in the winter which is taken as clouds by the satellite methods used by the 3 products. This means that sunny days with snow coverage are considered as cloudy days which lead to an under-estimation of the irradiance. An example is given in figure 6. Since the new generation of METEOSAT launched in August 2002, offers spectral channels which allow differentiating snow coverage from clouds, this problem will not happen on irradiance data estimated from satellite images of 2003.

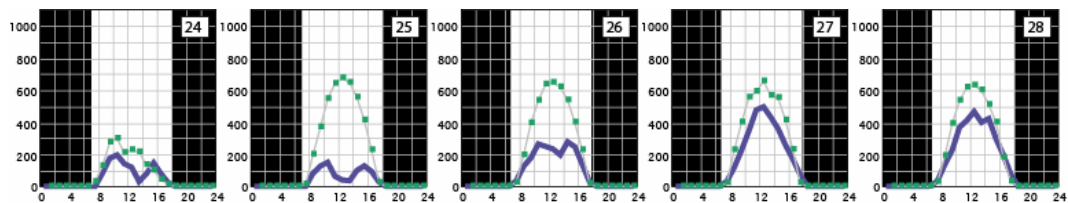


Figure 6: Davos, February 1999, example of a situation where sunny days with snow cover (ground measurements, dotted curves) are considered as cloudy days by the satellite estimates (plain curve).

The overall RMSD is 28% for SOLEMI and 20% for SATEL-LIGHT and ENMETSOL. In Davos, the RMSD is twice as much as in the other sites for the reasons explained above.

An overall value for the KSI cannot be given, as it would need an overall reference distribution, which is very difficult if the distributions for the stations are very different. The KSI values can only be compared individually. Each product obtains a KSI below 100% on 7 sites out of 10; this means a good match of frequency distributions. There are sometimes significant differences between products; this is the case of Geneva, Thessaloniki or Vaulx. SATEL-LIGHT is the product which provides the lowest KSI value across all sites, followed by ENMETSOL then SOLEMI.

The following figures present the large scale MESOR benchmarking which focused on the yearly sum of the global horizontal irradiation coming from eight products: EnMetSol, ESRA, HelioClim-2, Meteonorm 6, NASA SSE6, PVGIS, Satel-Light and SOLEMI. The irradiation from one product is compared to the average of the eight products using the relative difference.

Yearly sum of global horizontal irradiation: average of all databases [kWh/m2]

(databases: EnMetSol, ESRA, HelioClim-2, Meteonorm 6, NASA SSE 6, PVGIS, Satel-Light, SOLEMI)

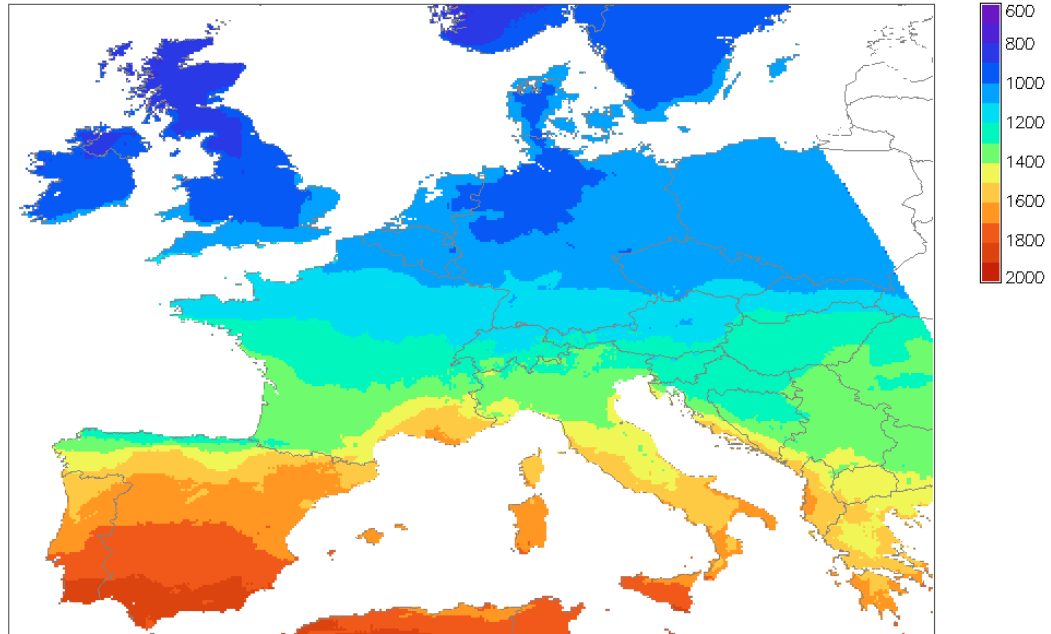


Figure 7: Yearly sum of global horizontal irradiation, average of eight products: EnMetSol, ESRA, HelioClim-2, Meteonorm 6, NASA SSE6, PVGIS, Satel-Light and SOLEMI.

Yearly sum of global horizontal irradiation: relative difference 'EnMetSol-average' [%]

(databases: EnMetSol, ESRA, HelioClim-2, Meteonorm 6, NASA SSE 6, PVGIS, Satel-Light, SOLEMI)

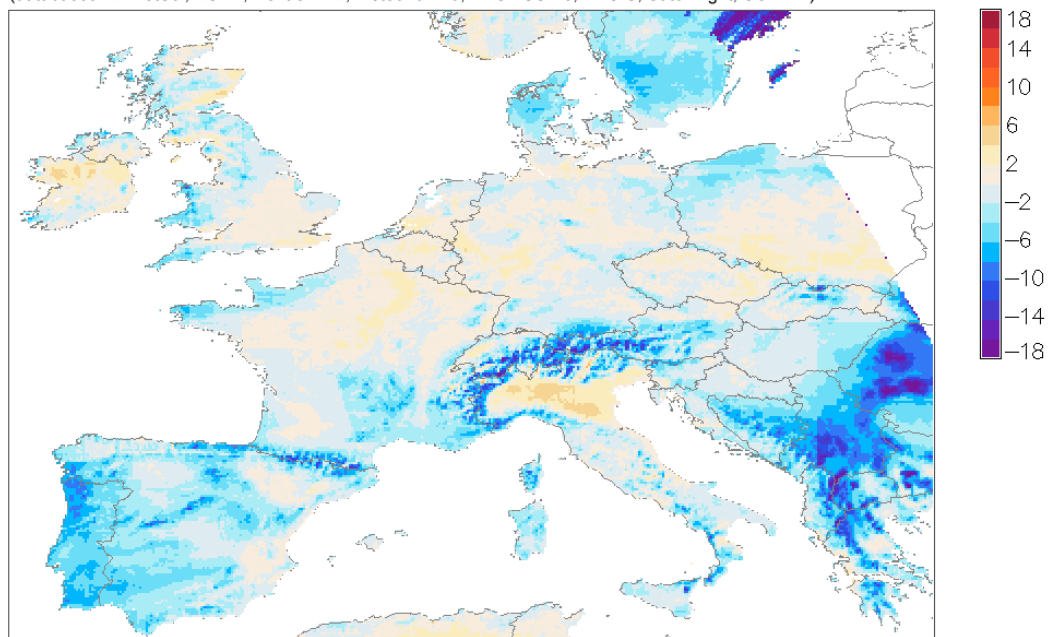


Figure 8: Difference in yearly sum of global horizontal irradiation between EnMetSol and the average of the eight products.

Yearly sum of global horizontal irradiation: relative difference 'ESRA-average' [%]

(databases: EnMetSol, ESRA, HelioClim-2, Meteonorm 6, NASA SSE 6, PVGIS, Satel-Light, SOLEMI)

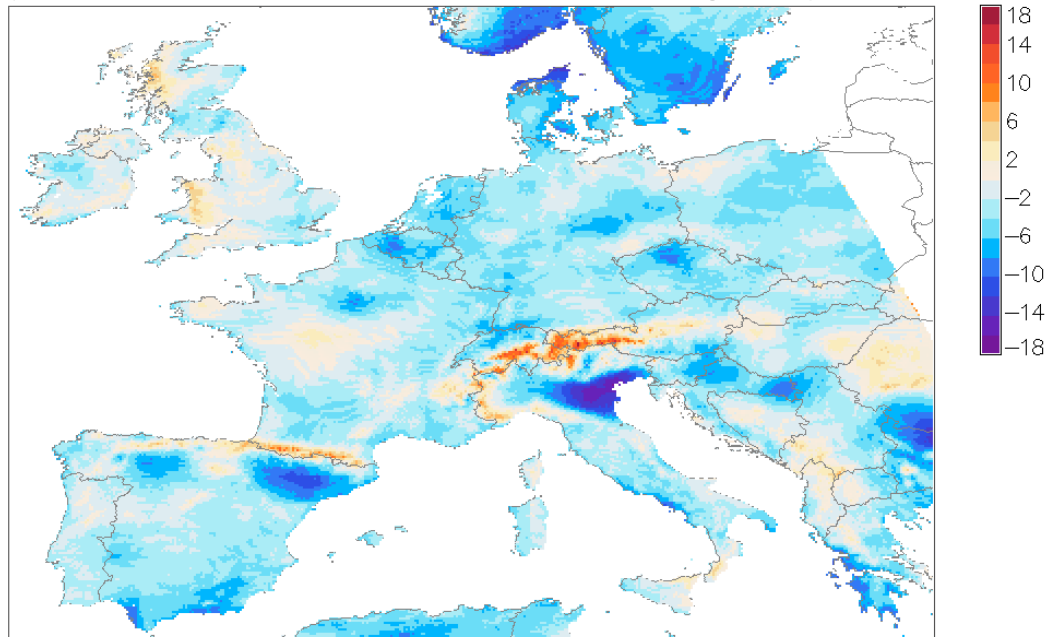


Figure 9: Difference in yearly sum of global horizontal irradiation between ESRA and the average of the eight products.

Yearly sum of global horizontal irradiation: relative difference 'HelioClim2-average' [%]

(databases: EnMetSol, ESRA, HelioClim-2, Meteonorm 6, NASA SSE 6, PVGIS, Satel-Light, SOLEMI)

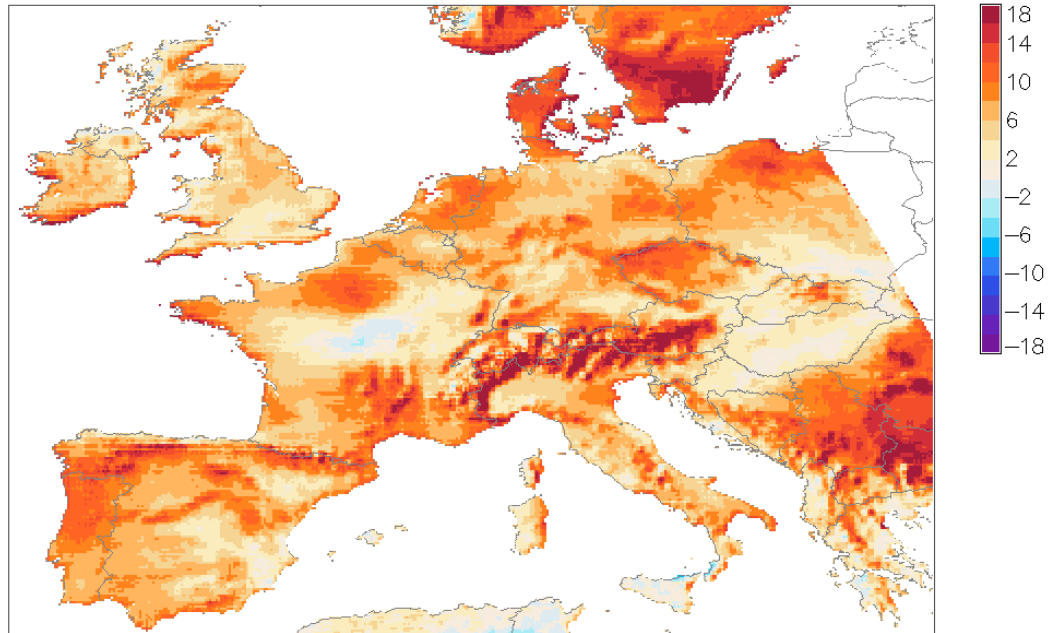


Figure 10: Difference in yearly sum of global horizontal irradiation between HelioClim-2 and the average of the eight products.

Yearly sum of global horizontal irradiation: relative difference 'Meteonorm6-average' [%]
(databases: EnMetSol, ESRA, HelioClim-2, Meteonorm 6, NASA SSE 6, PVGIS, Satel-Light, SOLEMI)

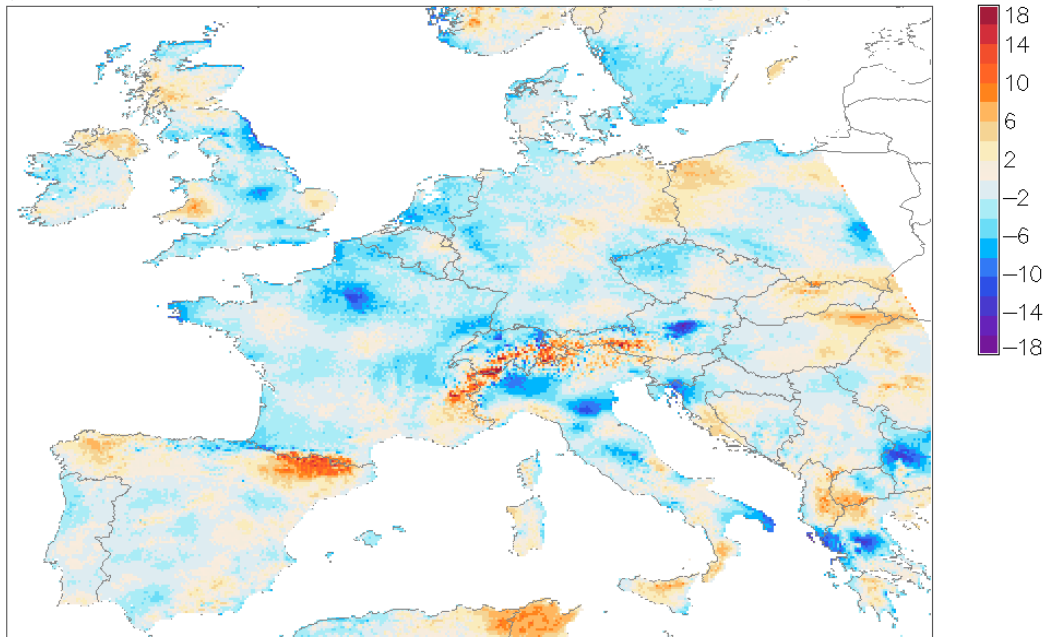


Figure 11: Difference in yearly sum of global horizontal irradiation between Meteonorm 6 and the average of the eight products.

Yearly sum of global horizontal irradiation: relative difference 'NASA SSE 6-average' [%]
(databases: EnMetSol, ESRA, HelioClim-2, Meteonorm 6, NASA SSE 6, PVGIS, Satel-Light, SOLEMI)

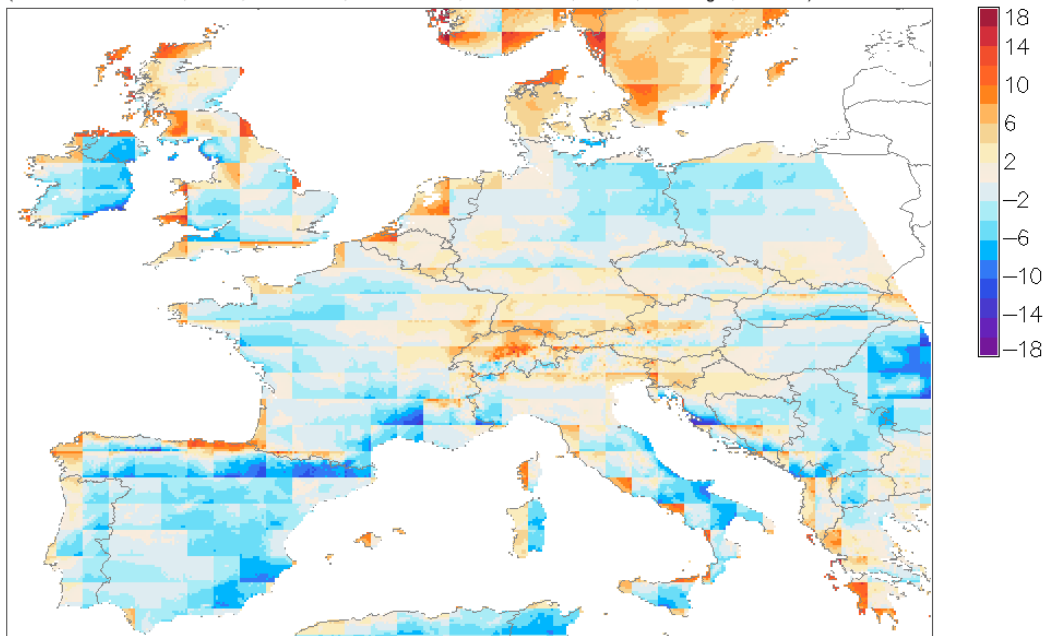


Figure 12: Difference in yearly sum of global horizontal irradiation between NASA SSE 6 and the average of the eight products.

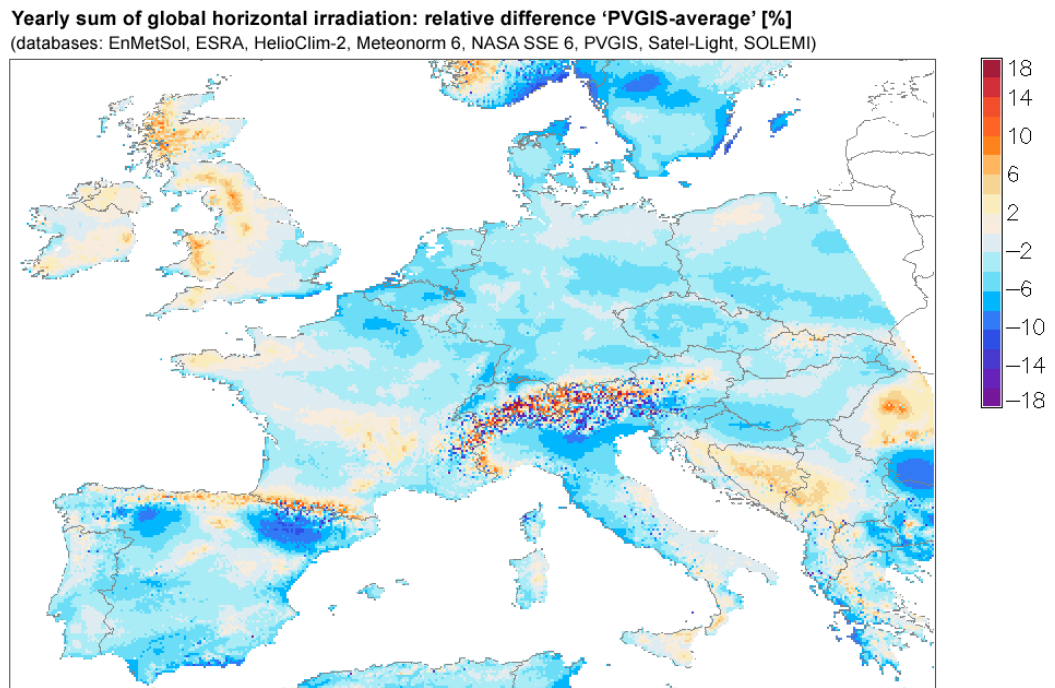


Figure 13: Difference in yearly sum of global horizontal irradiation between PVGIS and the average of the eight products.

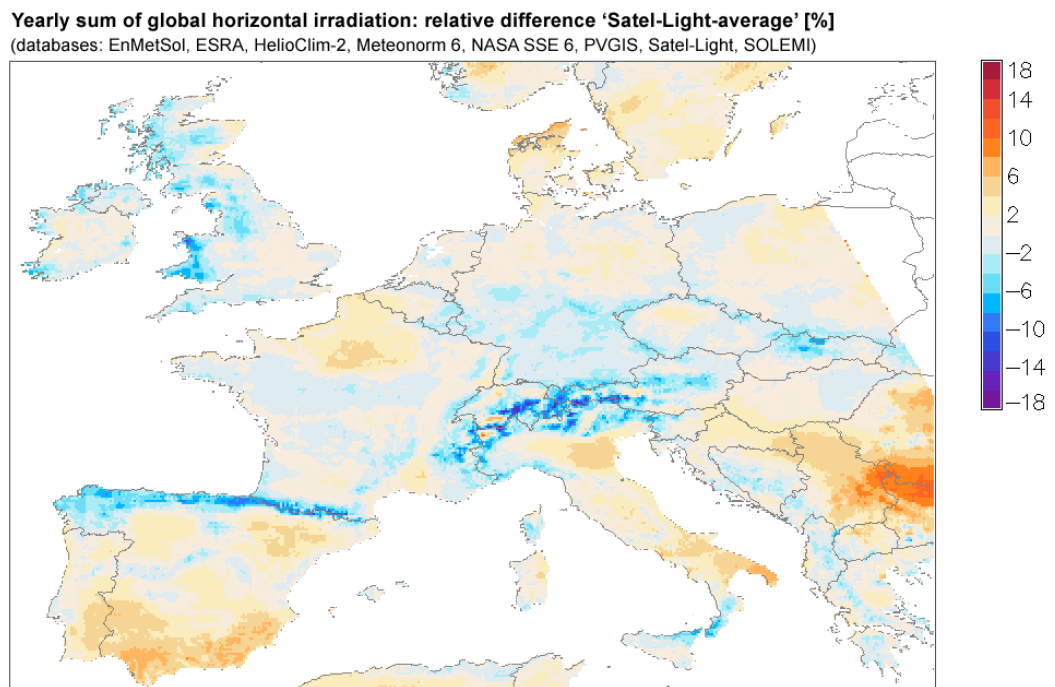


Figure 14: Difference in yearly sum of global horizontal irradiation between Satel-Light and the average of the eight products.

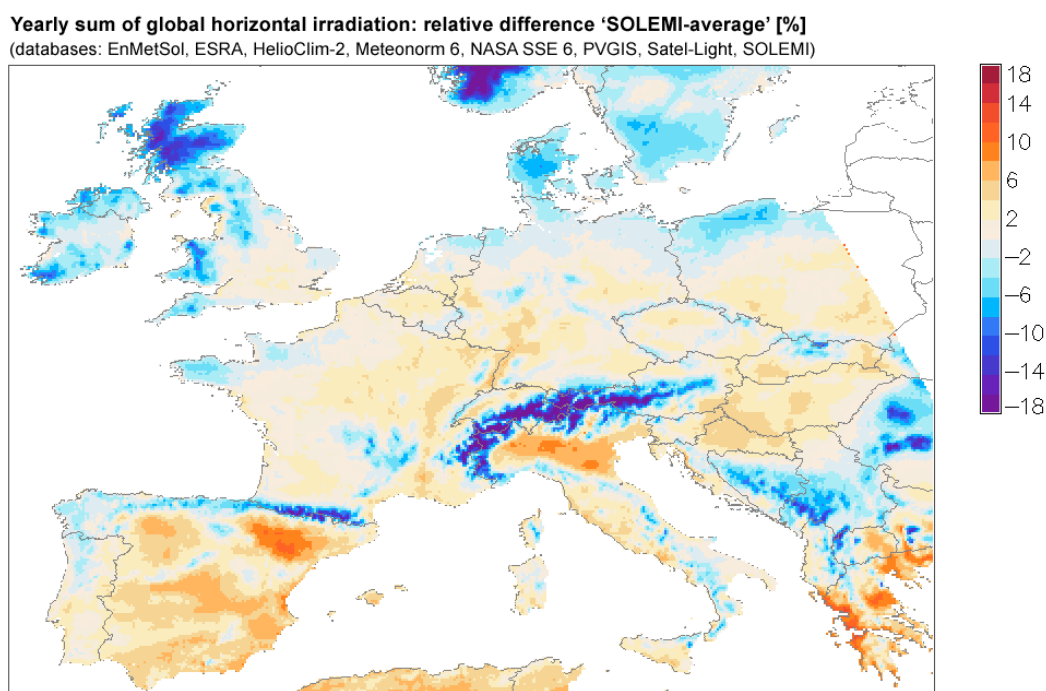


Figure 15: Difference in yearly sum of global horizontal irradiation between SOLEMI and the average of the eight products.

From the previous figures, we see that the products based on the interpolation of ground measurements provide overall lower irradiation values than the ones based on satellite estimates. Figure 9 (ESRA), figure 11 (METEONORM), figure 13 (PVGIS) exhibit large areas of negative difference with the average (blue areas). Products based on satellite images: EnMetSol, Satel-Light and SOLEMI, tend however to underestimate the solar radiation over mountainous areas; we have seen before that one reason comes from the influence of snow coverage. The data products which use high resolution terrain models: Meteonorm, PVGIS, better represent the complex patterns of solar radiation in mountainous regions. Data sets with low spatial resolution will very likely ignore regional patterns of the solar resource especially in mountainous and coastal zones.

The differences observed in the products lie in the differences in the methods: interpolation of ground measurements vs. processing of satellite images. The products depending on ground measurements are sensitive to the quality and completeness of the measurements (especially those from older time periods) and the density of the measuring stations (which is not satisfactory in many regions). The satellite based methods are affected by the higher uncertainty in the cloud cover assessment due essentially to a ground covered by snow or ice and to low sun angles. Additional differences also come from differences in time coverage (inter-annual variability), aerosol and water vapour databases, and complex terrain and climate conditions specific to mountains and coastal zones. There is certainly space for improvement in the models and in the data used as inputs to the models. We have tried to gather our ideas on future research objectives in deliverable D.1.3. We see also from this benchmarking that there is a clear need of high quality ground measurements in some areas where we have observed large differences between products.

3.2 *Direct normal irradiance*

Figure 16 gives the average hourly direct normal irradiance (DNI) obtained from the ground measurements. DNI was not measured at all sites for the period of time considered (figure 1). So, there is no value for Nantes, Thessaloniki and Vaulx. Payerne is the site where the average DNI is the highest followed by Carpentras and Davos. The lowest value is observed in Lindenberg.

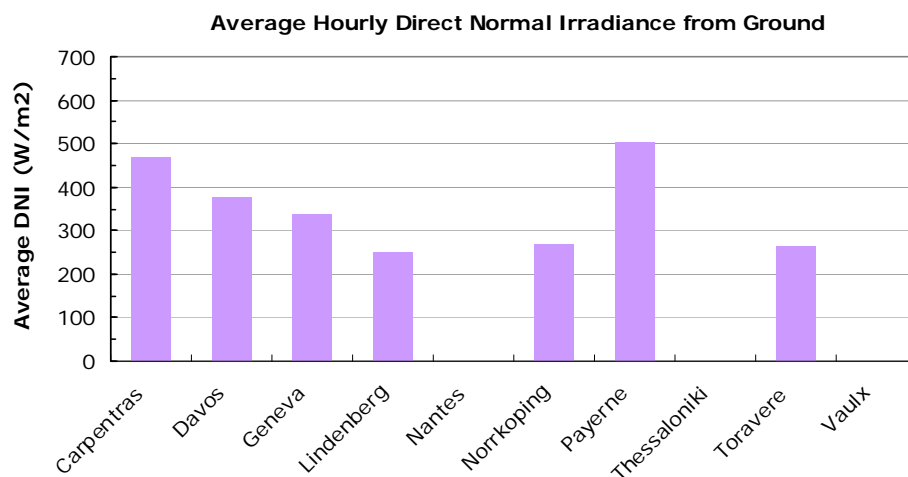


Figure 16: Average DNI for the benchmarking period (ground measurements).

The next 3 figures present the bias, the RMSD and the KSI obtained from the comparison between 3 solar resource products (ENMETSOL, SATEL-LIGHT, SOLEMI) and the ground measurements.

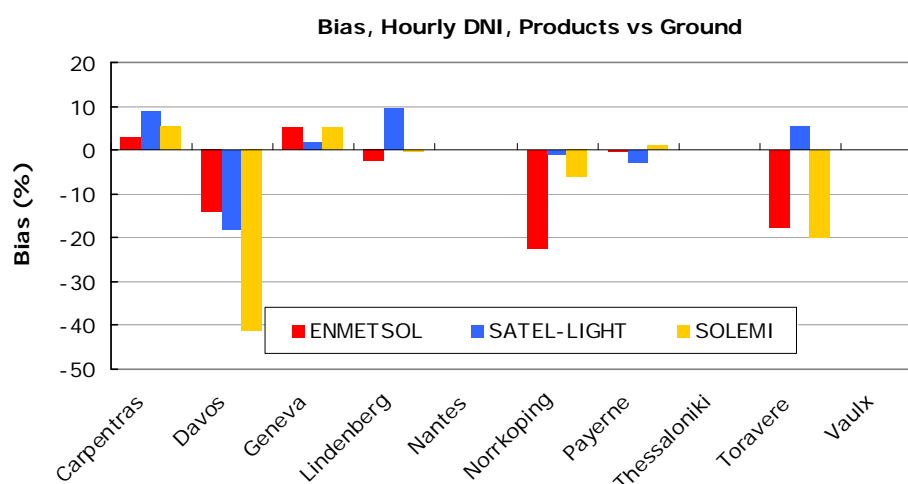


Figure 17: Bias between ground measurements and 3 products.

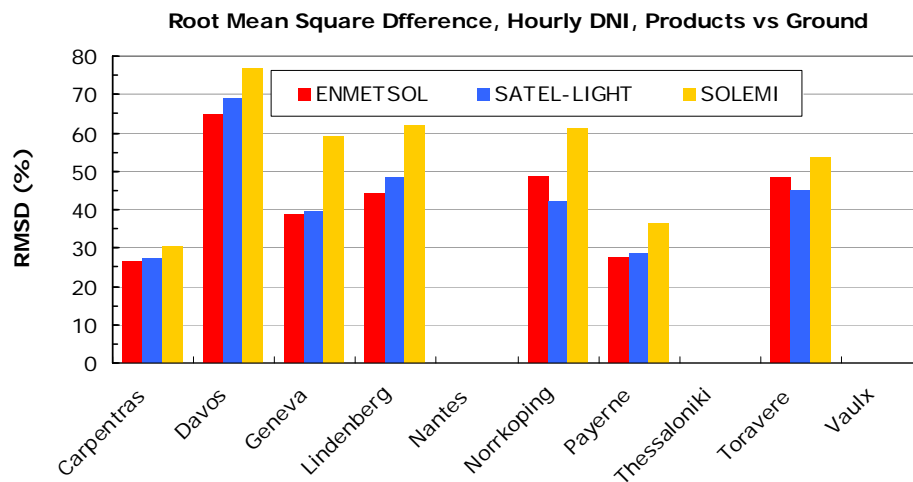


Figure 18: RMSD between ground measurements and 3 products.

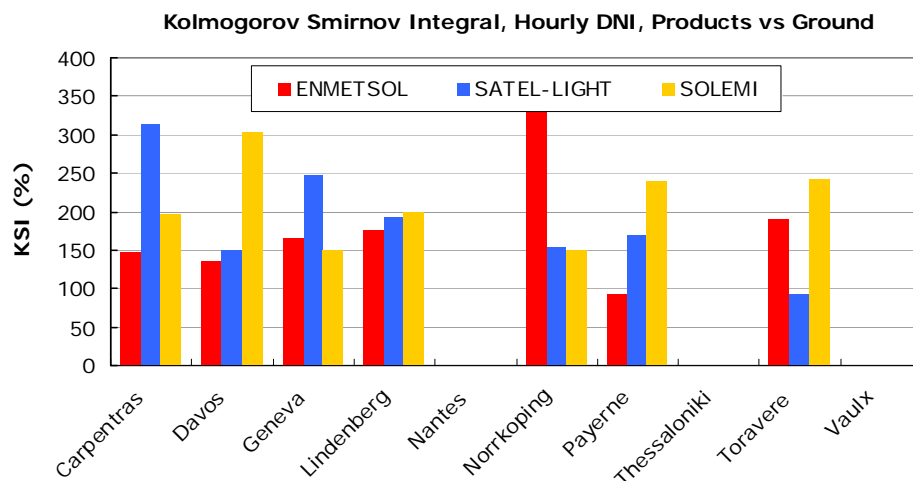


Figure 19: KSI between ground measurements and 3 products.

The overall bias is low: 1% for SOLEMI, 4% for SATEL-LIGHT and -1% for ENMETSOL. The RMSD is 48% for SOLEMI and 36% for SATEL-LIGHT and ENMETSOL. This is almost twice as much as for the global horizontal irradiance. This time KSI values are above 100% which means that it is difficult to match the frequency distribution of DNI measured on ground. Locally DNI is very much dependent on the position of clouds with respect to the sun. The improved resolution of satellite images (1 km instead of 5 km for SATEL-LIGHT), and improved information on cloud types will improve the determination of DNI.

The following figures present the large scale MESOR benchmarking which focused on the yearly sum of the direct normal irradiation coming from five products: METEONORM 6, NASA SSE6, PVGIS, SATEL-LIGHT and SOLEMI. The irradiation from one product is compared to the average of the other five as it was done for the global horizontal irradiance. The results are presented using the relative difference, i.e. the relative standard deviation expressed in %.

Figure 20 shows the average of the yearly sum of direct normal irradiation from the five databases. There are three regions of high yearly sum of DNI in Europe (values above 1800 kWh/m²) - Southern and Central Spain and Portugal, Sicily and Sardinia (Italy), and Provence (France). Although the variability of the database estimates in these areas, given by the relative standard deviation, stays generally within 7 to 8%, it increases in some regions such as the Mediterranean islands. The DNI resource in the rest of Italy and South-Eastern Europe is lower, and on top of this, the user's uncertainty from comparing values in different databases is often high (standard deviation reaching 20%). As for GHI, the figures showing the relative difference between one product and the average of the five are presented in the order from overall under-estimation to over-estimation of the average values.

Yearly sum of direct normal irradiation: average of all databases [kWh/m2]

(databases: Meteonorm 6, NASA SSE 6, PVGIS, SateI-Light and SOLEMI)

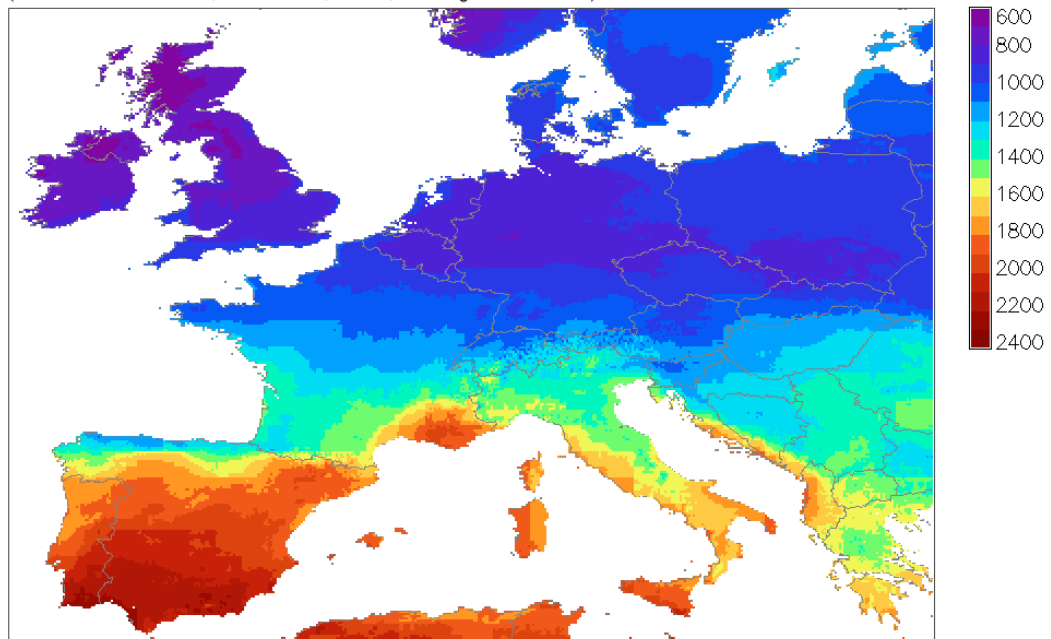


Figure 20: Yearly sum of direct normal irradiation, average of five products: METEONORM 6, NASA SSE6, PVGIS, SATEL-LIGHT and SOLEMI.

Yearly sum of direct normal irradiation: relative difference 'PVGIS-average' [%]

(databases: Meteonorm 6, NASA SSE 6, PVGIS, Satel-Light and SOLEMI)

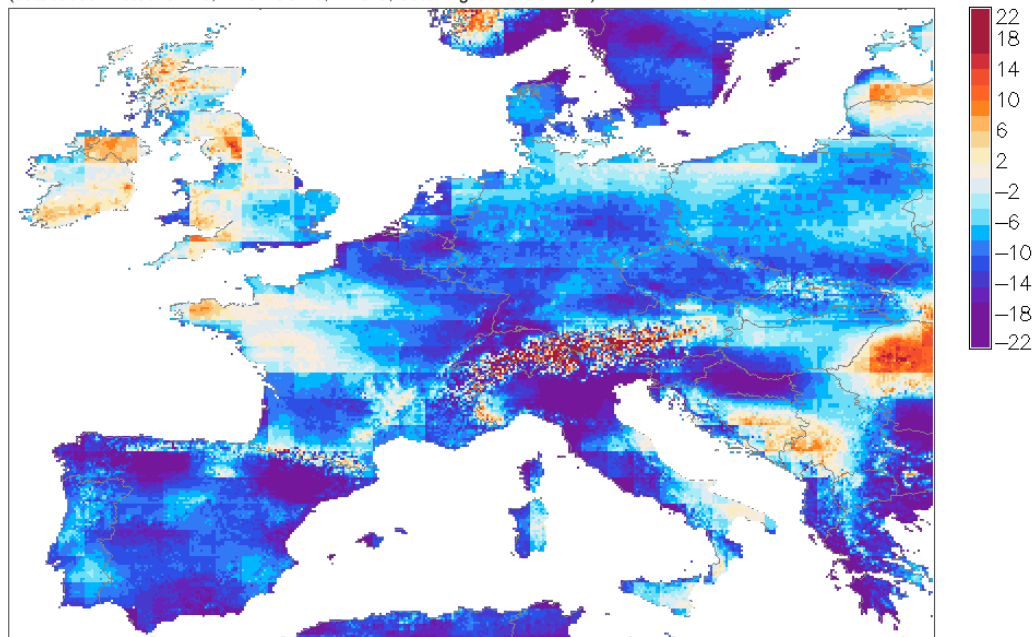


Figure 21: Relative difference in yearly sum of direct normal irradiation between PVGIS and the average of five products.

Yearly sum of direct normal irradiation: relative difference 'Meteonorm-average' [%]

(databases: Meteonorm 6, NASA SSE 6, PVGIS, Satel-Light and SOLEMI)

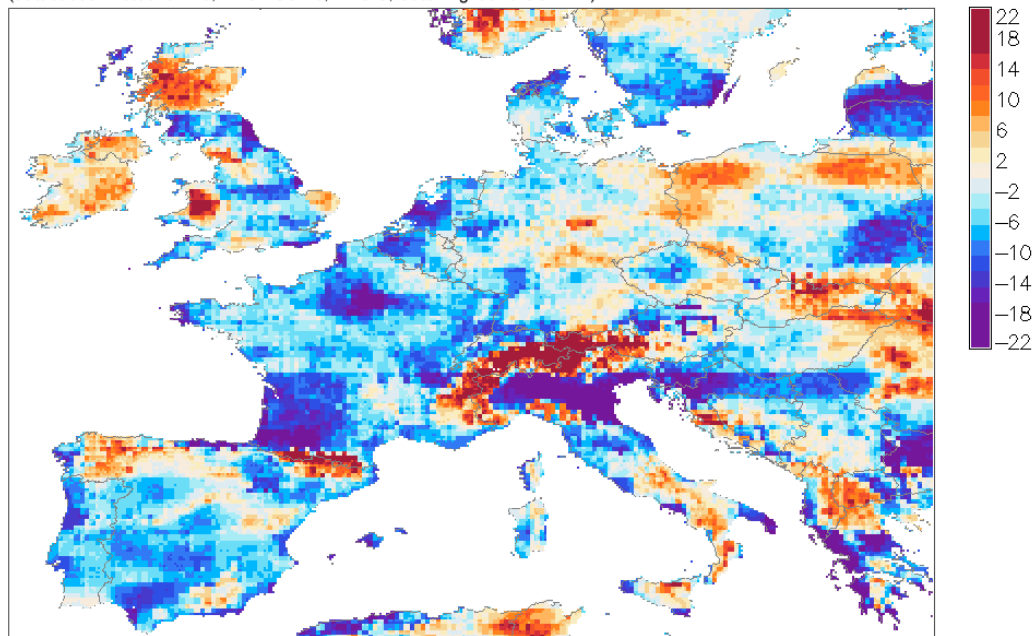


Figure 22: Relative difference in yearly sum of direct normal irradiation between METEONORM 6 and the average of five products.

Yearly sum of direct normal irradiation: relative difference 'SOLEMI-average' [%]
(databases: Meteororm 6, NASA SSE 6, PVGIS, Satel-Light and SOLEMI)

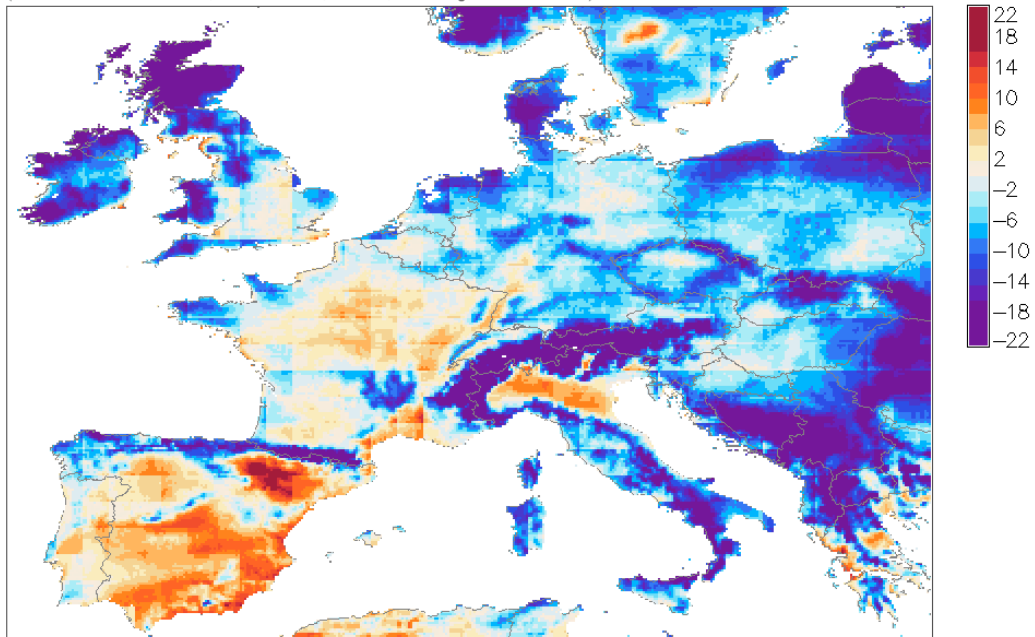


Figure 23: Relative difference in yearly sum of direct normal irradiation between SOLEMI and the average of five products.

Yearly sum of direct normal irradiation: relative difference 'Satellight-average' [%]
(databases: Meteororm 6, NASA SSE 6, PVGIS, Satel-Light and SOLEMI)

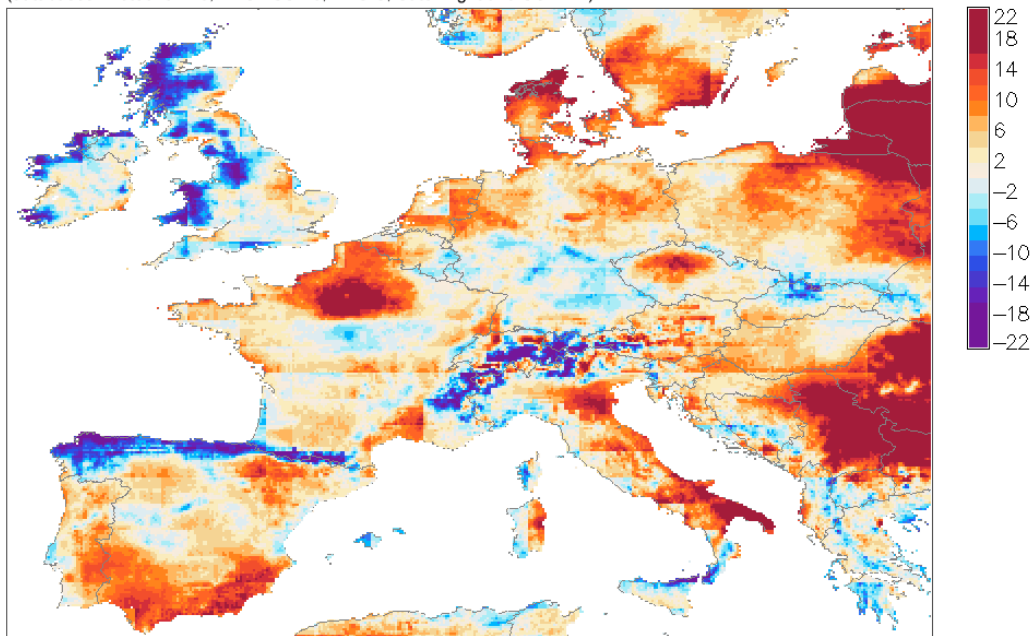


Figure 24: Relative difference in yearly sum of direct normal irradiation between SATELLIGHT and the average of five products.

Yearly sum of direct normal irradiation: relative difference 'NASA SSE6-average' [%]
(databases: Meeonorm 6, NASA SSE 6, PVGIS, Satel-Light and SOLEMI)

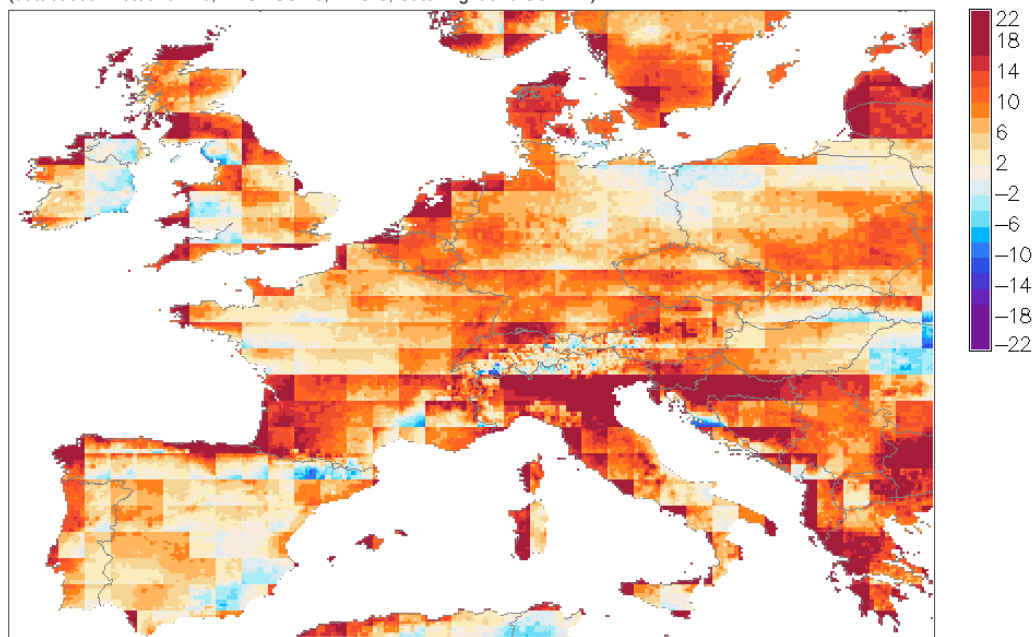


Figure 25: Relative difference in yearly sum of direct normal irradiation between NASA-SSE6 and the average of five products.

From the previous figures, we see that the higher disagreement between the products can be found in mountains (the Alps, Pyrenees, Carpathians, Balkan Mountains, etc.), but also along some coastal zones and even in flat regions of South and North-East Spain, around the Baltic and North Seas. High standard deviation shows strong disagreement between databases in Bulgaria and Romania, in Lithuania, South Scandinavia, and in the Po plain in Italy.

In the NASA SSE product, different equations for latitudes North and South from 45 degrees are used, and this results in sudden change in the DNI values. Very high deviations between all databases in the Balkan countries and Lithuania region may result from using different aerosol and atmospheric turbidity climate values and less accurate estimation of clouds by satellite algorithms.

Mountainous regions show high variability due to the fact that the terrain effects are considered at higher spatial resolution only in METEONORM and PVGIS. As explained before, the DNI estimates from satellite datasets result in higher uncertainty in mountains also due to difficulties in separation between clouds and snow as they are based on the older generation satellites.

DNI is more sensitive to the atmospheric parameters than GHI. The quality and the spatial detail of DNI estimates are determined by the input data used in the models: mainly parameters describing the optical state of the atmosphere, such as the Linke atmospheric turbidity, or the analytical datasets (ozone, water vapor, and aerosols). Like cloudiness, the state of the atmosphere is highly variable over time and space. Its measurement requires sophisticated instrumentation and complex satellite models which are only now becoming available. Because of this, most existing products use monthly averaged values from years in the past, which cannot represent the values of yesterday, today or tomorrow. Figure 26 gives an example of how different from the ground measurement a daily DNI estimate can be when using one monthly value.

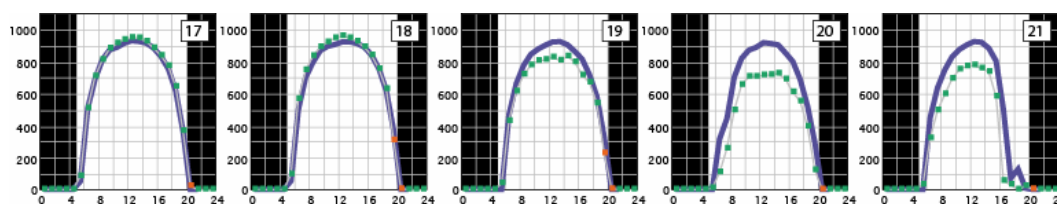


Figure 26: Carpentras, July 1998, DNI, example of a series of sunny days with variable atmospheric conditions. Ground measurements are shown with dotted curves, satellite estimates with plain curves. The monthly turbidity value used to compute the estimates is appropriate for 17 and 18, it is too high for 19, 20, 21.

The difference in atmospheric information also explains why even though SOLEMI and SATEL-LIGHT use the same type of data inputs (METEOSAT first generation); they still show differences in some regions.

4 References

- [Aguiar, 1988] R. J. Aguiar, M. Collares-Pereira and J. P. Conde, «Simple procedure for generating sequences of daily radiation values using a library of Markov transition matrices». Solar Energy, Vol. 40, N°3, pp. 269-279 (1988).
- [Beyer, 1997] H.G. Beyer, G. Czeplak, U. Terzenbach and L. Wald, « Assessment of the method used to construct clearness index maps for the new European Solar Radiation Atlas (ESRA)». Solar Energy, Vol. 61, N°6 (1997).
- [Czeplak, 1996] A. Skartveit, J.A Olseth, G. Czeplak and M. Rommel, « On the estimation of atmospheric radiation from surface meteorological data ». Solar Energy, Vol. 56, N°4 (1996).
- [Collares-Pereira, 1979] M. Collares-Pereira and A. Rabl, «On the estimation of atmospheric radiation from surface meteorological data». Solar Energy, Vol. 22, N°2 (1979).
- [Collares-Pereira, 1992] R. Aguiar and M. Collares-Pereira, «TAG: A time-dependent, autoregressive, Gaussian model for generating synthetic hourly radiation». Solar Energy, Vol. 49, N°3 (1992).
- [Duffie/Beckman 1991] J.A. Duffie, W.A. Beckman, Solar engineering of thermal processes (second edition), John Wiley & Sons. New York. 920 p (1990).
- [Dumortier, 1995] D. Dumortier, « Mesure, Analyse et Modélisation du gisement lumineux. Application à l'évaluation des performances de l'éclairage naturel des bâtiments », Thèse de Doctorat, Génie Civil et Sciences de l'Habitat, Université de Savoie, Chambéry (1995).
- [Erbs, 1982] D.G. Erbs, S.A. Klein and J.A. Duffie, «Estimation of the diffuse radiation fraction for hourly, daily and monthly-average global radiation». Solar Energy, Vol. 28, N°4, pp293-302 (1982).

- [Hammer, 2007] A. Hammer, E. Lorenz, D. Heinemann, «Fernerkundung der Solarstrahlung für Anwendungen in der Energietechnik» DACH 2007, Hamburg, Germany (2007).
- [Hammer, 2003] A. Hammer, D. Heinemann, C. Hoyer, R. Kuhlemann, E. Lorenz, R. Müller and H.G. Beyer, «Solar energy assessment using remote sensing technologies», Remote sensing of Environment, Vol. 86, N°3 (2003).
- [Hoyer-Click, 2009] C. Hoyer-Klick, H.G. Beyer, D. Dumortier, M. Schroedter-Homscheidt, L. Wald, M. Martinoli, C. Schilings, B. Gschwind, L. Menard, E. Gaboardi, J. Polo, T. Cebecauer, T. Huld, M. Suri, M. de Blas, E. Lorenz, C. Kurz, J. Remund, P. Ineichen, A. Tsvetkov, J. Hofierka, «MESoR - Management and Exploitation of Solar Resource Knowledge», Solar Paces 2009 Conference, Berlin (2009).
- [Kemper, 2008] A. Kemper, E. Lorenz, A. Hammer & D. Heinemann «Evaluation of a new model to calculate direct normal irradiance based on satellite images of Meteosat Second Generation», Eurosun2008, Lisbon, Portugal (2008).
- [Liu, 1960] B. Y. H. Liu, R. C. Jordan, «The interrelationship and characteristic distribution of direct, diffuse and total solar radiation». Solar Energy, Vol. 4, N°3, pp1-19 (1960).
- [Müller, 2004] R.W. Müller, P. Ineichen, M. Schroedter, S. Cros, K.F. Dagestad, D. Dumortier, R. Kuhlemann, J.A. Olseth, C. Piernavieja, C. Reise, L. Wald and D. Heinemann, «Rethinking satellite based solar irradiance modelling. The SOLIS clear sky module», Remote sensing of Environment, Vol. 91, N°2 (2004).
- [Muneer, 1990] T. Muneer, «Solar radiation model for Europe», Building Services Engineering Research and Technology, Vol. 11, 153-163 (1990).
- [Olseth, 1986] A. Skartveit and J. A. Olseth, «Modelling slope irradiance at high latitudes». Solar Energy, Vol. 36, N°4, pp181-188 (1986).
- [Perez, 1991] M. Vazquez, V. Ruiz and R. Perez, «The roles of scattering, absorption, and air mass on the diffuse-to-global correlations». Solar Energy, Vol. 47, N°3, pp181-188 (1991).
- [Perez, 1990] R. Perez, P. Ineichen, R. Seals, J. Michalsky and R. Stewart, «Modelling daylight availability and irradiance components from direct and global irradiance». Solar Energy, Vol. 44, N°5, pp271-289 (1990).
- [Perez, 1987] R. Perez, R. Seals, P. Ineichen, R. Stewart and D. Menicucci, «A new simplified version of the perez diffuse irradiance model for tilted surfaces». Solar Energy, Vol. 39, N°3, pp221-231 (1987).
- [Pinker, 1992] R.T. Pinker, I. Laszlo, «Modelling surface solar irradiance for satellite applications on global scale». J. Appl. Met. N°3, pp194-212 (1992).
- [Polo, 2009] J. Polo, B. Espinar, L. Ramírez, A. Drews, H.G. Beyer, L.F. Zarzalejo, L. Martín, «Analysis of different comparison parameters applied to solar

- radiation data from satellite and German radiometric stations ». *Solar Energy* 83, N°1, 118-125 (2009).
- [Rigollier, 2004] C. Rigollier, M. Lefèvre and L. Wald, «The method Heliosat-2 for deriving shortwave solar radiation from satellite images ». *Solar Energy* 77, N°2, 159-169 (2004).
- [Remund, 1998] J. Remund, E. Salvisberg, S. Kunz, « On the generation of hourly shortwave radiation data on tilted surfaces » *Solar Energy*, Vol. 62, N°5, pp331-344 (1998).
- [Remund, 2003] J. Remund, L. Wald, , M. Lefèvre, T. Ranchin, J. Page, « Worldwide Linke turbidity information ». Proceedings of the ISES Solar World Congress 2003, Göteborg, Sweden, 16-19 June (2003).
- [Skartveit, 1998] A. Skartveit, J.A. Olseth and M.E. Tuft, « An hourly diffuse fraction model with correction for variability and surface albedo », *Solar Energy*, 63, N°3, pp 173-183 (1998).
- [Skartveit, 1986] A. Skartveit, J.A. Olseth, « Modeling slope irradiance at high latitudes », *Solar Energy*, 36, N°4, pp. 333-344 (1986).
- [Suri, 2004] M. Šúri and J. Hofierka, « A new GIS-based solar radiation model and its application to photovoltaic assessments », *Transactions in GIS*, N°8, pp 175-190 (2004).
- [Suri, 2009] M. Šúri, J. Remund, T. Cebecauer, C. Hoyer-Klick, D. Dumortier, T. Huld, P.W. Stackhouse, P. Ineichen « Comparison of Direct Normal Irradiation Maps for Europe », *Solar Paces 2009 Conference*, Berlin (2009).
- [Zelenka, 1992] V. D'Agostino and A. Zelenka, «Supplementing solar radiation network data by co-kriging with satellite images». *Int. Jour. of Climatology* 12, pp. 749-761 (1992).

5 Examples of use

This section provides 20 case studies showing how solar resource data is being used in real life. Each case study has been provided by a stakeholder, then drafted by a member of the MESOR consortium and finally edited by ENTPE. The MESOR consortium thanks all the contributors of the case studies for having taken time to share their experience with their use of solar resource data.

Case studies have been designed for quick reading, they only have two pages. They focus on the study and its use of solar radiation data. For the readers who want more technical details, there is a contact/link section at the end of each case study. These case studies cover different fields of use:

- Photovoltaic systems
- Solar thermal systems
- Concentrating Solar Power systems
- Solar forecasting
- Daylighting and Buildings
- Solar bio treatment